Single-Chain Fv-Streptavidin Substantially Improved Therapeutic Index in Multistep Targeting Directed at Disialoganglioside GD2

Nai-Kong V. Cheung, MD, PhD[1]; Shakeel Modak, MD[1]; Yukang Lin, PhD[2]; Hongfen Guo, MS[1]; Pat Zanzonico, PhD[3]; John Chung, MD[1]; Yuting Zuo[2]; James Sanderson[2]; Sibylle Wilbert[2]; Louis J. Theodore, PhD[2]; Donald B. Axworthy, PhD[2]; and Steven M. Larson, MD[3]

[1]*Department of Pediatrics, Memorial Sloan-Kettering Cancer Center, New York, New York;* [2]*NeoRx Corporation, Seattle, Washington; and* [3]*Department of Nuclear Medicine, Memorial Sloan-Kettering Cancer Center, New York, New York*

Multistep targeting can improve the therapeutic index of antibody-based targeting, particularly relevant to pediatric tumors where acute toxicity and late effects of treatment are major concerns. Neuroblastoma is uniquely suited for such investigations because of its abundance of surface ganglioside GD2. **Methods:** 5F11scFv (scFv = single-chain variable fragment) was constructed from the variable regions of the heavy (V_H) and κ-light (V_L) chain complementary DNA (cDNA) of anti-GD2 IgM hybridoma 5F11 and ligated to full-length streptavidin cDNA for expression in *Escherichia coli*. Purified 5F11-scFv-streptavidin (5F11-scFv-SA) was a homotetramer and showed comparable avidity to 5F11 IgM and a 30-fold improvement over monomeric scFv. Biodistribution of 5F11-scFv-SA was studied in nude mice xenografted with neuroblastoma LAN-1. Twenty-four hours after intravenous injection of 300–900 μg 5F11-scFv-SA, 150–450 μg of a thiogalactoside-containing clearing agent, $(Gal\text{-}NAc)_{16}$-α-S-C_5H_{10}-NH-LC-N-Me-biotin (molecular weight, 8,652), were administered intravenously, followed by ~2.5 μg (1.85–3.7 MBq) ^{111}In-1,4,7,10-tetraazacyclododecane-1,4,7,10-tetraacetic acid-biotin (^{111}In-DOTA-biotin) intravenously 4 h later and clocked as time 0. **Results:** Tumor uptake (percentage of injected dose per gram [%ID/g]) at 2 h was 7 %ID/g and decayed with a half-life of 72 h, whereas blood %ID/g rapidly decreased to <1/500 of that of tumor after the first 24 h. The tumor-to-nontumor (T/NT) ratio at 72 h was high (median, 106; range, 3.4 [kidney] to 1,660 [blood]). When the area under the radioactivity curve was computed, the T/NT organ ratio was favorable (4.8 for kidney and 162 for blood). When human and murine tumors were surveyed, the T/NT ratio of ^{111}In-DOTA-biotin uptake correlated with their levels of GD2 expression as assayed by flow cytometry. Biotinylated polypeptides (bovine serum albumin and vasointestinal peptides) achieved selective tumor targeting when the multistep strategy was applied. **Conclusion:** Improvement in the T/NT ratio using pretargeting strategy may increase the efficacy and safety of scFv-based approaches in cancer therapy. Additionally, since biotinylated polypeptides can be rendered tumor selective, a large repertoire of agents can potentially be explored.

Received Aug. 30, 2003; revision accepted Nov. 21, 2003.

For correspondence or reprints contact: Nai-Kong V. Cheung, MD, PhD, Department of Pediatrics, Memorial Sloan-Kettering Cancer Center, 1275 York Ave., New York, NY 10021.

E-mail: cheungn@mskcc.org.

Key Words: single-chain variable fragment; scFv-streptavidin; multistep targeting; dosimetry; biodistribution

J Nucl Med 2004; 45:867–877

Gangliosides are acidic glycosphingolipids found on the outer surface of most cell membranes. They are concentrated in gray matter and synaptic junctions in the nervous system, especially during brain development (*1*). In serum, gangliosides are found in low concentrations (e.g., GD2 is <10 pmol/mL) and are transported by selective lipoproteins. Only trace amounts of gangliosides are found in the cerebrospinal fluid. The lipophilic ceramide portion of the ganglioside is inserted into the lipid bilayer of membranes and the hydrophilic carbohydrate moieties are exposed to the external environment. In vivo, gangliosides are comparatively stable with biologic half-lives ($t_{1/2}$) of 34–38 d in retinal cells. GD2 is found in a wide spectrum of human tumors, including neuroblastoma (NB), osteosarcomas, soft-tissue sarcomas, medulloblastomas and high-grade astrocytomas, melanomas, and small cell lung cancer (*2–4*). GD2 is a potential target for monoclonal antibodies (mAbs) because of the high antigen density, lack of modulation, and relative homogeneity in NB. In contrast, the only normal tissues with high ganglioside expression are restricted to tissues of the central nervous system and some peripheral nerves. Several anti-GD2 antibodies have been produced by the hybridoma technique. Clinical experience of anti-GD2 antibody has so far been collected primarily in patients with NB, where both murine (3F8, 14G2a) and chimeric (14.18) mAbs have been used. Tumor imaging studies in patients consistently demonstrated selective tumor uptake with a very favorable tumor-to-nontumor (T/NT) ratio (*2*). Clinical antitumor effects were evident with both naked antibody and radiolabeled antibodies (*5*).

Single-chain variable fragments (scFv) are genetic fusion proteins consisting of the variable regions of the heavy (V_H) and κ-light (V_L) chains from mAbs (*6,7*). scFv can be linked

to other bioactive proteins for targeting to tumors. scFv-streptavidin (scFv-SA) (*8,9*) is expected to have clinical utility for pretargeting biotin-conjugated radioisotopes, drugs, toxins, enzymes, and cytokines. The utility of increased valency and specificity with improved binding avidity can now be clinically explored. The 2-step targeting approach (*9–14*) separates the administration of the antibody from the cytotoxic ligand, thus decoupling the slow blood clearance and tumor-targeting kinetics of the antibody from the potentially fast kinetics of the ligands. GD2 (on NB) is ideal for the multistep targeting (MST) strategy since (a) the majority of the antigen is retained on the cell surface after antibody binding and (b) the density of this antigen is relatively high (5×10^6 molecules per NB cell). scFv-SA is one example of how pretargeting may improve therapeutic ratios. Here we describe the first successful construction and expression of an anti-GD2 scFv-SA fusion protein, its in vitro and in vivo characterization, and its targeting potential for radioisotopes and polypeptides.

MATERIALS AND METHODS

Tumor Cell Lines

Established human cell lines were cultured in 10% defined calf serum (Hyclone) as previously described (*15*). Additional lines of NB include SK-N-JD and SK-N-LP from Memorial Sloan-Kettering Cancer Center (MSKCC); and colon carcinoma Colo205, lymphoma Daudi, leukemia MOLT-4, and rhabdomyosarcoma HTB82 from the American Type Culture Collection. Murine melanoma cell lines B16D14, B16D14Kb, and B16D14KbKd were provided by Dr. Kenneth Lloyd of MSKCC.

Preparation of 5F11-scFv-SA

The variable regions of the heavy (V_H) and κ-light (V_L) chains were amplified by polymerase chain reaction (PCR) separately from complementary DNA (cDNA) of the hybridoma 5F11 and an assembled scFv fragment was cloned into a vector to form the plasmid 5FpCE18 (*16*). The V_L fragment of 5F11 was further subcloned from the 5FpCE18 plasmid by PCR with primer pair RX1499 (CGGCGGCTCG AGCGACATCG AGCTGACTCA GTCTCCAGCA ATCATG) and RX1504 (GAGCCAGAGC TCTTGATTTC CAACTTTGTC CCAGCA), subsequently treated with *Xho* I and *Sac* I restriction enzymes, and cloned into a vector (E171-5-21) to form the plasmid G113-1-1. The V_H fragment was subcloned by 2 steps of "sewing" PCR from the 5FpCE18 with the primer pairs (step 1: RX1495 [GAATTCCCAT GGCTCAGGTT CAGCTGCAGC AGTCAGGACCT] and RX1496 [GCTCTT-TCCG TGGCTCTGCT TCACCCAGTGC]; RX1497 [AAGCA-GAGCC ACGGAAAGAG CCTTGAGTGGATT] and RX1498 [CACCAGAGAT CTTGGAGACG GTGACCGTGG TCCCT]; step 2: RX1495 and RX 1498) and cloned into the vector E171-5-21, digested with *Nco* I–*Bgl* II, to form the plasmid G108-2-3. An *Eco*RI–*Xho* I fragment of G108-2-3 was ligated into a vector, G113-1-1, digested with *Eco*RI–*Xho* I, to give plasmid G116-1-13. An *Eco*RI–*Sst* II fragment of 5F11-scFv containing a 25-mer $(GGGGS)_5$ between V_H and V_L was excised from the plasmid G116-1-13 and inserted into E31-2-20 plasmid between a streptavidin coding region and signal sequence (*17*) to form G119-1. The G119-1 plasmid expressed the 5F11-scFvSA fusion gene and exhibited kanamycin resistance in *Escherichia coli* (XL1-Blue). The coding sequence of the matured scFvSA fusion protein encoded 417 amino acids with a predicted monomeric molecular weight (M_r) of 43,179 and a tetrameric M_r of 172,716. Anti-CD20 B9E9 scFv-SA was previously described (*17*), and anti-TAG-72 CC49 scFv-SA was provided by NeoRx Corp. The method of fermentation of 5F11-scFv-SA in a BioFlow 3000 fermentator (New Brunswick Scientific) was similar to the one previously described for B9E9 scFv-SA (*17*).

The expression level of the 5F11-scFv-SA fusion protein was monitored by a rhodamine-biotin high-performance liquid chromatography (HPLC) assay (*17*) during the fermentation, and the culture was harvested at 39 h after inoculation. The purification of 5F11-scFv-SA was based on a modification of a method previously described (*17*). The final product was exhaustively dialyzed in phosphate-buffered saline (PBS) at 4°C. After sterile filtration, the fusion protein was stored at 5°C at a concentration of ≤1 mg/mL. Alternatively, the deaggregated fusion protein was concentrated at 5°C to 3–5 mg/mL in PBS containing 5% sorbitol and stored at −70°C. Purified scFvSA fusion protein was analyzed by sodium dodecyl sulfate–polyacrylamide gel electrophoresis (SDS-PAGE) under nonreducing conditions with or without heating at 95°C for 10 min in the SDS loading buffer. It was also analyzed by size-exclusion HPLC (*17*). For mass analysis of monomeric 5F11, liquid chromatographic separation was conducted with a Hewlett Packard series 1100 system fitted with a polyhydroxyethyl aspartamide column (200 × 9.4 mm, 5 μm, 1,000 Å; PolyLC Inc.) operated in the size-exclusion mode.

Competitive Inhibition Assays

Serial dilutions of 5F11-scFv (*16*) or 5F11-scFv-SA allowed inhibition of the binding of anti-5F11 antiidiotypic antibody 1G8 to 5F11 in an enzyme-linked immunosorbent assay using a modification of the method previously described (*15,18*).

Synthetic Clearing Agent (sCA)

The sCA, provided by NeoRx Corp., consists of a bifunctional moiety with multiple *N*-acetyl-galactosamine residues linked to biotin ($M_r \sim 8{,}652$) (*13,19*). The sCA binds rapidly to the circulating scFv-SA fusion protein. The resulting complex clears rapidly from the circulation into the liver by the asialogalactose receptor present on hepatocytes (*13,19*).

Radiolabeling

One-half microliter (2–5 μg) of 1,4,7,10-tetraazacyclododecane-1,4,7,10-tetraacetic acid-biotin (DOTA-biotin) (NeoRx Corp.) dissolved in H_2O (*13,20*) was reacted with 38.7 μL (22.2 MBq) $^{111}InC1_3$/HCl (PerkinElmer Life and Analytical Sciences Inc.), in 194 μL of 2 mol/L ammonium acetate as previously described (*17*). The specific activity of ^{111}In-DOTA-biotin was 0.75 ± 0.23 MBq/μg. scFv-SA fusion proteins, antibody 3F8, biotinylated bovine serum albumin ([BSA], Sigma-Aldrich), biotinylated porcine intestinal peptide (PHI), and biotinylated vasoactive intestinal peptide ([VIP], Peninsula Laboratories, Inc.) were radiolabeled with ^{125}I as previously described (*21*). For biodistribution studies, the average specific activities were 0.30, 0.37, 0.30, 1.48, and 1.33 MBq/μg, respectively. For scintigraphy studies with BSA, PHI, and VIP, the average specific activities were 0.15, 0.41, and 0.48 MBq/μg, respectively.

^{111}In-DOTA-Biotin Binding Assessment

Avidin agarose beads (Sigma-Aldrich) were mixed by vortexing for 20 s, and 200 μL were dispensed into a Rainin tube upper

chamber (0.2 or 0.45 μm, part 7016-021, Nylon-66) before spinning at 10,000*g* for 2 min. The filtrate was discarded and the beads were resuspended in 300 μL PBS by vortexing. Centrifugation and washing were repeated twice. After discarding the filtrate, beads were finally resuspended in 300 μL PBS by vortexing. Two to 5 μL ^{111}In-DOTA-biotin preparations were added, vortexed for 10 s, and allowed to incubate at room temperature for 5 min, before centrifugation at 10,000*g* for 2 min. The beads were then washed twice with 300 μL PBS, retaining all filtrates. The percent binding to avidin beads was calculated using the formula: (100 − [100 × [cpm in filtrate/total cpm applied to beads]]). The percent binding (mean ± SD; $n = 12$ experiments) was 97.6% ± 0.7%.

Pretargeting Technique

Tumor-bearing mice were injected intravenously with 300–900 μg of 5F11-scFv-SA (1.7–5.2 nmol) for pretargeting. After 24 h were allowed for distribution and tumor localization, 150–450 μg (17.3–52 nmol) of sCA were injected intravenously to clear circulating 5F11-scFv-SA from the blood. Four hours after injection of the sCA, 2–5 μg (2.2–5.5 nmol) ^{111}In-DOTA-biotin (1.63 ± 0.19 MBq) was injected intravenously (time 0). Five to 7 d before pretargeting, the mice were started on a low-biotin diet (biotin-deficient PD1RR; Test Diet) to reduce the endogenous biotin level. An average dose of 0.41 MBq ^{125}I-3F8 was injected intravenously for biodistribution studies. For biodistribution studies of ^{125}I-labeled fusion proteins, BSA, PHI, and VIP, the average dose per mouse was 3.78, 1.78, 1.11, and 1.07 MBq, respectively. For scintigraphy studies, the average dose per mouse was 1.15, 1.37, and 1.81 MBq, respectively. Mice were anesthesized with ketamine and imaged with an ADAC Vertex Plus γ-camera system. For ^{125}I, the collimation used was comprised of two 6:1 ratios, 60-lines-per-inch (2.54 cm) linear Bucky grids overlaid on one another with septa of one perpendicular to the septa of the other. An average of ~10^5 counts acquired per image. For late imaging (e.g., day 10 after injection), mice were killed before scintigraphy.

Tumor Model

Outbred athymic mice were purchased from National Cancer Institute Frederick Cancer Center. CB-17 SCID-Beige mice were from Taconic, and C57Bl/6 mice were from Jackson Laboratory. Tumor cells were planted (1–5 × 10^6 cells) subcutaneously in 100 μL of Matrigel (BD BioSciences). Experiments were performed under Institutional Animal Care and Use Committee–approved protocols, and institutional guidelines for the proper and humane use of animals in research were followed. After implantation, tumor sizes (maximum orthogonal diameter) were measured. Experiments were initiated when tumor sizes reached 9.3 ± 1.6 mm in diameter, usually by 21 d of tumor implantation, in groups of 5 mice per cage. Mice were injected intravenously (retrorbital plexus) with radiolabeled antibody, fusion protein, or biotin-DOTA. They were killed at indicated time points, and their organs were removed, weighed, and counted in a universal γ-counter (Packard Bioscience). For scintigraphy, they were first anesthesized intraperitoneally with ketamine (Fort Dodge Animal Health) and imaged at indicated time points with a γ-camera (ADAC) equipped with grid collimators.

Statistics

In biodistribution studies, the primary endpoints of these comparisons were the percentage of injected dose per gram (%ID/g) and T/NT ratios. From pilot studies, to allow for a maximum of 30% SEM in 98% of these estimates, 4 or 5 mice per group were chosen for each experimental time point. To compute a composite relationship of the T/NT ratio to the dose of 5F11-scFv-SA or the sCA, the T/NT ratio across all organs was normalized using the mean and variance across the various dose levels. The mean normalized T/NT ratio (for all organs and for a set of critical organs) at each dose level was tested for significance using the Student *t* test.

Absorbed-Dose Calculations

Normal tissue and tumor radiation absorbed doses in tumor-bearing mice were determined for ^{131}I-3F8 and for ^{90}Y-DOTA-biotin based on the time-dependent biodistributions (%ID/g) of their surrogate radiotracers, ^{125}I-3F8 and ^{111}In-DOTA-biotin. ^{111}In is a commonly used surrogate to estimate ^{90}Y dose. Using the numeric module of the SAAM II simulation, analysis, and modeling program (*22*), the time–activity data for each tissue were fitted to a 1-component, a 2-component, or more complex exponential functions as appropriate. The resulting time–activity functions were then analytically integrated to yield the cumulated activity concentration per unit administered activity (MBq-h/g per MBq injected) in each tissue. The absorbed dose per unit administered activity (cGy/MBq) was calculated first by assuming the dose to each tissue was due only to β-ray self-irradiation—that is, the dose contributions from γ-rays (in the case of ^{131}I) and from other tissues were ignored. Furthermore, the initial absorbed-dose estimates for both ^{131}I and ^{90}Y were derived assuming complete local absorption of the β-rays—that is, assuming that all β-ray energy emitted within a particular tissue was completely absorbed within that tissue. This is the standard assumption used for β-ray dosimetry, at least in humans (*23*). However, since a significant portion of the more-penetrating ^{90}Y β-rays escapes from source regions of the size of mouse organs, the assumption of complete local absorption may not be valid (*24*). Accordingly, a second method of ^{90}Y tissue absorbed-dose calculation used a scaling factor based on the absorbed fraction for electrons with an energy equal to the average ^{90}Y β-ray energy (0.94 MeV) in unit-density spheres having the same mass as the respective tissue. The ^{90}Y β-ray absorbed fractions thus ranged from as low as 0.20 for the mouse bladder plus contents (which averaged 0.010 g in mass in our model) to 0.84 for the mouse tumors (4.2 g). Our liver and kidney absorbed-dose estimates based on this scaling approach agreed very well with those calculated using the self-irradiation S factors of Kolbert et al. (*25*). The self-irradiation absorbed fractions for the much less-penetrating ^{131}I β-rays (average energy, 0.19 MeV) were all well over 0.9; therefore, the ^{131}I β-ray absorbed fractions based on the complete local-absorption assumption were considered accurate.

RESULTS

Expression, Purification, and Characterization

Fermentor-produced 5F11-scFv-SA fusion protein was purified from homogenized *E. coli* cell extracts to >95% homogeneity on a single iminobiotin affinity column. The recovery for the fusion protein was about 86%, with <9% appearing in the flow-through or wash. The residual remained as entrapped material on the column. The iminobiotin-purified fusion protein displayed 25% aggregate, which was subsequently reduced to 7.4% by treating with urea. HPLC size-exclusion chromatography indicated that the deaggregated fusion protein exhibited a major peak with a

retention time appropriate for the tetramer (8.06 min). The deconvoluted mass spectrum of the purified fusion protein (43,158 Da) agreed with the calculated average mass (43,179 Da) for the mature monomeric subunit. In the SDS–PAGE gel, 5F11-scFv-SA migrated as a tetramer of ~172 kDa that dissociated to a monomer (43 kDa) on heating. These data indicated that the fusion protein was secreted properly into the periplasm of *E. coli* cells, where it spontaneously formed a tetramer. In addition, by western blot analysis, antiidiotypic antibody 1G8 reacted with both the monomer and the tetramer (data not shown).

In vitro binding assays have shown that 5F11-scFv-SA bound avidly to GD2 (solid-phase purified antigen or cell bound) and to the antiidiotypic antibody 1G8. Though 5F11-scFv-SA and 5F11 were equivalent in inhibiting binding of 1G8 to 5F11, 5F11-scFv monomers were at least 10-fold less efficient (data not shown). In addition, biotinylated ligands (e.g., phycoerythrin and fluorescein isothiocyanate) bound strongly to these molecules. When radiolabeled with ^{125}I, its blood clearance in nontumor-bearing mice had a $t_{1/2}$ α of 0.2 h, and $t_{1/2}$ β of 9.3 h (Table 1). These half-lives were shorter than expected, when compared with those of anti-CD20-scFv-SA (B9E9) ($t_{1/2}$ α, 0.7 h; $t_{1/2}$ β, 13.4 h) or with those of anti-CC49-scFv-SA ($t_{1/2}$ α, 0.4 h; $t_{1/2}$ β, 14.0 h).

In Vivo Biodistribution

Athymic nude mice xenografted with established human NB LAN-1 (0.5- to 0.8-cm diameter) were injected intravenously with 5F11-SA, followed in 24 h by an intravenous injection of the sCA biotin-LC-NM-(gal-NAc)$_{16}$, and then 4 h later injected with ~2.5 μg (3.1 nmol) ^{111}In-DOTA-biotin. In the first series of experiments, 4 dose levels of 5F11-SA were tested: 100 μg (0.59 nmol), 300 μg, 900 μg, and 2,400 μg (5 animals per group). The dose of sCA was 50% (by weight) of the 5F11-scFv-SA dose. For each organ, the T/NT ratio was summarized in Table 2. To compute a composite relationship of the T/NT ratio to dose, an average T/NT ratio across all organs was calculated by first normalizing these ratios using the mean and variance across the four 5F11-scFv-SA dose levels. The mean ± SEM of the normalized T/NT ratio, when plotted against 5F11-scFv-SA dose, plateaued at 900 μg for both the T/NT ratio and the %ID/g in tumor. It was true when all organs were used in the normalized calculations and when only critical organs (brain, blood, heart, liver, lung, kidney, spleen, and small intestines) were considered (Fig. 1). For both analyses, the normalized T/NT ratio at the 900-μg dose was significantly different ($P < 0.05$) from both the 300- and the 100-μg doses; 900 μg (5.3 nmol) was chosen as the standard dose for the remaining targeting studies. In the second series of experiments, using a fixed dose of 900 μg of 5F11-scFv-SA, the dose of sCA agent was titrated. Again, the mean ± SEM of the T/NT ratios was calculated (Table 3); when the ratios were mean and variance normalized across all organs, the optimal dose of sCA was determined to be 450 μg, when all organs were included in the normalized calculations, and when only critical organs (brain, blood, heart, liver, lung, kidney, spleen, and small intestines) were considered. For both analyses, the normalized T/NT ratio at the 450-μg (52 nmol) dose was comparable to that at 900 μg but was significantly better ($P < 0.05$) than the ratios at 300, 75, or 15 μg. Considering the fact that the tumor %ID/g did not significantly change with the dose of sCA (Table 3), 450 μg was chosen as the standard dose of sCA.

Scintigraphic Studies of 5F11-scFv-SA MST

Athymic mice xenografted with NB LAN-1 cells were imaged after dosing with 900 μg 5F11-scFv-SA, 450 μg of sCA, and ~2.5 μg of ^{111}In-DOTA-biotin. γ-Scintigraphy was performed 2 and 24 h after ^{111}In-DOTA-biotin injection. Rapid tumor uptake was apparent at 2 h with gut uptake of 4.2 %ID/g, which decreased to 0.6 %ID/g at 24 h (Fig. 2) and persisted for days (0.4 %ID/g on day 6). This early intestinal uptake occurred partly because of the biotin-free mouse chow, which contained avidin.

Biodistribution Studies for Dosimetry

Athymic mice with xenografted NB LAN-1 were injected with the standard dose of 900 μg 5F11-scFv-SA, 450 μg of sCA, and ~2.5 μg of ^{111}In-DOTA-biotin. Blood samples

TABLE 1
Blood Clearance of Fusion Proteins and Biotin-DOTA

scFv-SA	Biotinylated ligand	%ID/g		Half-life* (h)	
		30 min	20 h	$t_{1/2}$ α	$t_{1/2}$ β
^{125}I-5F11-scFv-SA	—	34.9	5.5	0.2 ± 0.1	9.3 ± 0.7
^{125}I-B9F9-scFv-SA	—	47.6	12.2	0.7 ± 0.1	13.4 ± 1.0
^{125}I-CC49-scFv-SA	—	35.2	10.1	0.4 ± 0.1	14.0 ± 0.9
5F11-scFv-SA					
300 μg	^{111}In-Biotin-DOTA	0.7	0.02	0.1 ± 0.01	4.6 ± 3.2
900 μg	^{111}In-Biotin-DOTA	1	0.02	0.14 ± 0.01	3.8 ± 0.7

*Mean ± SEM.

Blood clearance studies were carried out in tumor-free nude mice. Half-lives were calculated for the respective radiolabeled ligand using Origin 6.0 software (Microcal Software).

TABLE 2
Relationship of T/NT Ratio and Dose of scFv-SA

Tissue	Dose of 5F11-scFv-SA (μg)			
	100	300	900	2,400
Adrenal	19.7 ± 5.5	65.3 ± 20.3	124.6 ± 20.9	193.1 ± 7.1
Bladder	22.8 ± 4.3	29.1 ± 3.8	145.2 ± 44.4	92.1 ± 7.6
Blood	139.4 ± 30.3	160.9 ± 17.3	1,121.3 ± 306	621.4 ± 61.5
Brain	170.9 ± 12.6	503 ± 100.6	1187 ± 268	901.6 ± 157.4
Femur	67.3 ± 11	169.4 ± 27.1	405.2 ± 38.1	288.8 ± 41.9
Heart	34.3 ± 4	110.8 ± 13.3	265 ± 30.9	269.7 ± 11
Kidney	1.1 ± 0.3	2.7 ± 0.6	10.6 ± 2.9	7.1 ± 0.2
Large intestine	3.7 ± 1	17.4 ± 3.9	15.9 ± 3.2	10.2 ± 1.7
Liver	10 ± 1.6	18.5 ± 2.6	50.3 ± 11.9	37 ± 1.5
Lung	19.8 ± 3.1	21.8 ± 3.4	62.8 ± 21.5	23.1 ± 2.3
Muscle	35.8 ± 6.1	160.7 ± 22.9	467 ± 61.4	429 ± 39
Skin	13.3 ± 1.9	23.6 ± 4.4	51.4 ± 3.9	56.6 ± 8.3
Small intestine	37.4 ± 7	66 ± 9.2	135.6 ± 33.1	114.3 ± 24.9
Spine	49.2 ± 5.9	130.8 ± 20	425.4 ± 58.8	338.6 ± 27.2
Spleen	14.8 ± 2.2	30.8 ± 4.1	118.2 ± 12.3	120.2 ± 5.8
Stomach	48.2 ± 14.9	94.7 ± 12.4	181.7 ± 30.7	70.6 ± 5.2
Tumor %ID/g	1.9 ± 0.5	3.1 ± 0.9	6.5 ± 1.5	7.4 ± 0.5

T/NT ratio was calculated as follows: (%ID/g in tumor)/(%ID/g in tissue). Athymic nude mice xenografted with established human NB LAN-1 (0.5- to 0.8-cm diameter) were injected intravenously with 5F11-SA, followed in 24 h by intravenous injection of sCA biotin-LC-NM-(Gal-NAc)$_{16}$, and then 4 h later injected intravenously with ~2.5 μg ^{111}In-DOTA-biotin. Mice were killed 24 h after ^{111}In-DOTA-biotin for biodistribution studies. Four dose levels of 5F11-SA were tested: 100, 300, 900, and 2,400 μg (n = 5 mice per group). Dose of sCA was 50% (weight ratio) of 5F11-scFv-SA dose. T/NT ratio was summarized for each organ as arithmetic mean ± SEM.

were obtained for kinetic studies. At 2, 19, 52, 104, and 144 h, groups of mice (n = 5) were killed and their organ radioactivity was measured. The %ID/g for blood and various organs was calculated. DOTA-biotin had a rapid clearance from the blood in the first 5 h, irrespective of whether the xenograft was GD2 positive (LAN-1 NB) or GD2 negative (HTB82 rhadomyosarcoma). Tumor uptake peaked around 5 h and decayed with an effective $t_{1/2}$ of around 40 h. When compared with the blood radioactivity uptake, the differential was highly favorable (Fig. 3). The T/NT ratio from 2 to 144 h after ^{111}In-DOTA-biotin injection is shown in Table 4. Both median and mean ratios improved from 39 and 59 at 2 h to 159 and 359 at 52 h, respectively, and then decreased over time, except for the tumor-to-blood ratio, which continued to improve to >25,000 at 144 h. 5F11-scFv-SA was tested at 2 dose levels, 900 and 300 μg, with 450 and 150 μg of sCA, respectively. For comparison, ^{131}I-3F8 (a murine IgG3 anti-GD2 antibody currently in clinical trial (*2*)) was also tested at various time points in groups of 5 mice each. ^{131}I-3F8 was chosen because of its highly favorable therapeutic T/NT ratio and therapeutic results (*21,26*) in contrast to its radiometal conjugates (*27*) and specifically ^{111}In-DOTA-3F8, which showed substantial hepatic uptake and suboptimal tumor localization (data not shown). Based on the %ID/g, radiation absorbed doses were calculated as described. Though the typical tumor-to-blood radiation dose ratio for 3F8 was 2.7, the ratios for 5F11-scFv-SA MST were significantly better, 58 and 164, for the 300- and 900-μg scFv-SA dose, respectively (Table 5, model 1). Unlike ^{131}I-3F8, where myelosuppression was the dose-limiting toxicity, for ^{90}Y-DOTA-biotin renal toxicity could be a limiting factor. Using the absorbed fraction method, and using a kidney-to-kidney S factor of 222 cGy/

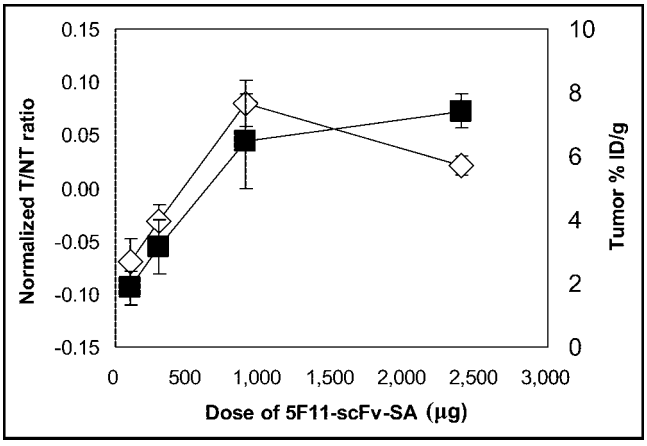

FIGURE 1. Relationship of normalized T/NT ratio and tumor uptake to dose of 5F11-scFv-DA. T/NT ratios across all organs in Table 1 were normalized using mean and variance across four 5F11-scFv-SA dose levels. Mean ± SEM of normalized T/NT ratio (◇) of critical organs (brain, blood, heart, liver, lung, kidney, spleen, and small intestines) were plotted against 5F11-scFv-SA dose. Average tumor uptake (%ID/g ± 1 SEM; ■) was also plotted for comparison. Normalized T/NT ratio at 900-μg dose was significantly different (P < 0.05) from those at 300- and 100-μg doses.

TABLE 3
Relationship of T/NT Ratio and sCA Dose

Tissue	Dose of sCA (μg)				
	15	75	300	450	900
Adrenal	32.1 ± 15.1	70.4 ± 18.3	97.3 ± 20.5	110.1 ± 21.2	183.7 ± 28.3
Bladder	34.8 ± 15.6	70.7 ± 24.6	56.7 ± 11.7	155.3 ± 54.5	159.5 ± 48.7
Blood	71.8 ± 43.3	277.1 ± 74.5	263.1 ± 75.2	1,040.2 ± 348.6	629 ± 177
Brain	427 ± 210.8	307.7 ± 70.9	807.9 ± 436.8	1,074.4 ± 362.8	860.5 ± 657.3
Femur	113.4 ± 78.4	344 ± 121.7	174.8 ± 34.4	394.6 ± 49.8	353.1 ± 49.5
Heart	78.9 ± 41.9	147.7 ± 25.1	201.7 ± 51.3	273.6 ± 55.7	208.2 ± 20.7
Kidney	1.3 ± 0.3	4 ± 0.8	3.6 ± 0.7	8 ± 2.9	6.8 ± 1
Large intestine	20 ± 8.3	24.1 ± 7.9	21.4 ± 7.4	13.2 ± 3.3	47.4 ± 19
Liver	18.6 ± 10	25.7 ± 4.4	32.3 ± 9.1	48.8 ± 14.7	32.6 ± 5.6
Lung	15.8 ± 8.9	19.5 ± 5.4	25.1 ± 4.7	43.5 ± 21.5	63.2 ± 23.4
Muscle	112.6 ± 53.3	153.7 ± 30.2	203.8 ± 59.8	432.8 ± 59.1	537.7 ± 104.4
Skin	19.1 ± 8.3	26.3 ± 8.6	40.7 ± 11.3	48.3 ± 4.7	58.9 ± 13.5
Small intestine	99.2 ± 52.3	130.4 ± 31.5	143.5 ± 37.8	166.3 ± 44.6	209.6 ± 51.4
Spine	71.2 ± 46.7	216.9 ± 58	221.3 ± 47	452.4 ± 86.4	371.8 ± 27.6
Spleen	18.9 ± 7.9	81.4 ± 15.8	98.4 ± 22.2	117.7 ± 21.2	130.3 ± 13
Stomach	38.4 ± 17.2	61.1 ± 9.5	173.1 ± 55.7	176.5 ± 39	260.7 ± 28.5
Tumor %ID/g	7.9 ± 2.4	6 ± 1.3	4.8 ± 0.9	6 ± 0.7	6.3 ± 3.2

T/NT ratio was calculated as follows: (%ID/g in tumor)/(%ID/g in tissue). Athymic nude mice xenografted with established human NB LAN-1 (0.5- to 0.8-cm diameter) were injected intravenously with 5F11-SA, followed in 24 h by intravenous injection of sCA biotin-LC-NM-(Gal-NAc)$_{16}$, and then 3 h later injected intravenously with ~2.5 μg ^{111}In-DOTA-biotin. Fixed dose of 900 μg of 5F11-scFv-SA was used at 5 doses of sCA (n = 4–8 mice per group). Mice were killed 24 h after ^{111}In-DOTA-biotin for biodistribution studies. T/NT ratio was summarized for each organ as arithmetic mean ± SEM.

MBq-h for ^{90}Y β-rays and a standard 0.18-g kidney (*25*), the kidney self-dose was 614 cGy, or only 54% of the kidney dose (at 300 μg 5F11-scFv-SA) based on the assumption of complete local absorption. The self-irradiation absorbed dose overestimate was likely to be more pronounced for distributed tissues such as blood. In Table 5, model 2, radiation absorption dose was recalculated using organ or tumor mass–dependent β-ray absorbed fractions modeling each organ or tumor as equivalent-mass unit-density spheres (*24*). The tumor-to-kidney radiation dose ratio was 4.0 at 300 μg and 4.8 at 900 μg of 5F11-scFv-SA.

Specificity of 5F11-scFv-SA MST to Human and Mouse Tumors

Mice xenografted with GD2-negative human lymphoma (Daudi), leukemia (MOLT-4), colon carcinoma (Colo 205), rhabdomyosarcoma (HTB82), and GD2-positive NB

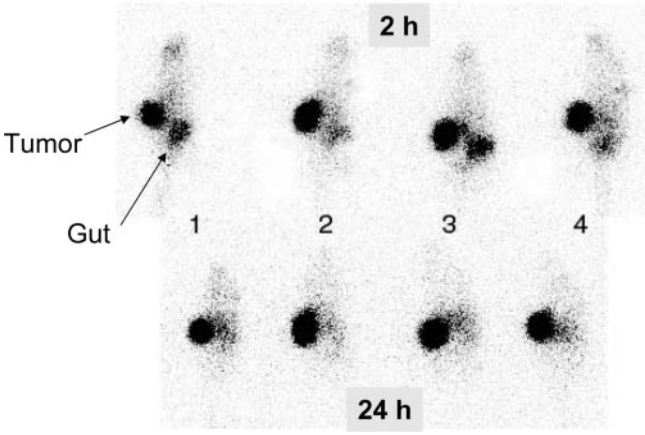

FIGURE 2. Scintigraphic studies of 5F11-scFv-SA MST. Athymic mice xenografted with NB LAN-1 cells were imaged after dosing with 900 μg 5F11-scFv-SA, 450 μg of sCA, and ~2.5 μg of ^{111}In-DOTA-biotin. γ-Imaging was performed 2 and 24 h after ^{111}In-DOTA-biotin injection. Maximal tumor diameters averaged 9 ± 1 mm.

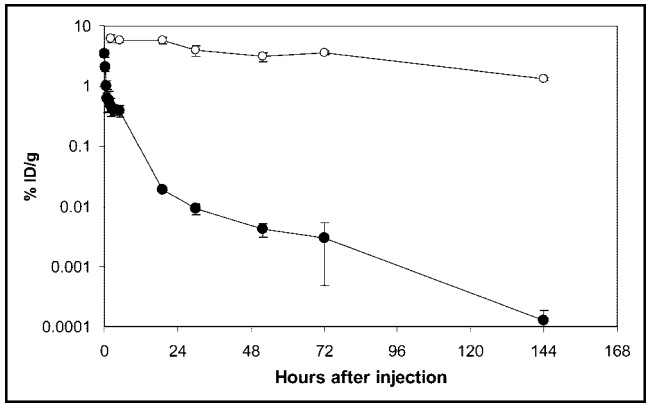

FIGURE 3. Comparison of blood vs. tumor decay in MST. Athymic mice (5 mice per group) with xenografted NB LAN-1 were injected with standard dose of 900 μg 5F11-scFv-SA, 450 μg of sCA, and ~2.5 μg of ^{111}In-DOTA-biotin. %ID/g for blood (●) and tumor (○) was calculated, showing a remarkable differential rapidly achieved within first 12 h after ^{111}In-DOTA-biotin injection.

TABLE 4
Relationship of T/NT Ratio and Time After Injection of Ligand

Organ	Time after injection of ^{111}In-DOTA-biotin (h)						
	2	5	19	30	52	72	144
Adrenal	34.6 ± 7.6	45.6 ± 20.2	50.8 ± 6.7	73.6 ± 24	172.9 ± 90.8	84.6 ± 30.3	69.4 ± 12.4
Bladder	32.3 ± 7.1	30.9 ± 9.5	74.2 ± 19.1	96.9 ± 42.3	75.9 ± 20.4	49.8 ± 16.1	39.5 ± 8.4
Blood	38 ± 8.8	60.8 ± 11.6	309.1 ± 53.6	442.3 ± 37.1	888.3 ± 242	1,661 ± 765.5	28,002 ± 12,082
Brain	106.4 ± 33.7	134.8 ± 44.2	490.6 ± 187.2	929.4 ± 745.9	378.9 ± 66.1	181.2 ± 69	460.2 ± 298.5
Femur	117.2 ± 20.3	254.7 ± 74.1	255.7 ± 59.7	221.1 ± 30.6	249.2 ± 39.6	171.9 ± 27.6	96.9 ± 16.7
Heart	94.5 ± 18.9	119.6 ± 26	183.7 ± 34.8	190.2 ± 41.4	111.6 ± 19	173.4 ± 25.3	66.6 ± 10.8
Kidney	6.7 ± 1.5	6.1 ± 1.6	5.8 ± 1.5	5.3 ± 2.5	4.2 ± 0.7	3.5 ± 0.4	2.4 ± 0.6
Large intestine	5.8 ± 2.1	3.3 ± 1	26.1 ± 6.3	31.4 ± 11.3	44.7 ± 6.8	60.7 ± 13.7	57.5 ± 14.9
Liver	28.3 ± 4.7	26.5 ± 6.1	34.5 ± 9.3	36.6 ± 10.5	30.9 ± 5.2	15.9 ± 3	13.2 ± 2.7
Lung	20.3 ± 2.5	20 ± 4.5	37.5 ± 7.2	41.5 ± 12.2	36.7 ± 5.3	23.2 ± 5.1	36 ± 8.2
Muscle	135.4 ± 34.5	180.3 ± 53.4	255 ± 56.1	224.7 ± 44.7	302.4 ± 53.4	208.8 ± 42.1	125.8 ± 33.8
Skin	32.2 ± 10.2	38.5 ± 7	68.2 ± 7.6	72.6 ± 5.7	34.4 ± 4	26.2 ± 4.3	24.4 ± 4.5
Small intestine	40.9 ± 11.8	34.5 ± 10.4	152.1 ± 37.8	196.7 ± 47.2	286.2 ± 66.8	216.4 ± 55.8	136.6 ± 20.6
Spine	129.2 ± 26.8	169.7 ± 37.4	182.5 ± 43.2	131.5 ± 20.4	372 ± 58.6	241.9 ± 23.4	109.9 ± 28.6
Spleen	79.2 ± 14.6	83.1 ± 18.7	92.4 ± 23.2	71.5 ± 14.6	63.2 ± 15	101.3 ± 22.9	16.6 ± 4.1
Stomach	65.4 ± 13.2	90.2 ± 22.3	139.5 ± 24.8	106.4 ± 37.3	159.4 ± 25.3	110.8 ± 30.7	93.3 ± 18.5

T/NT ratio was calculated as follows: (%ID/g in tumor)/(%ID/g in tissue). Athymic mice with xenografted NB LAN-1 were injected with standard dose of 900 μg of 5F11-scFv-SA, 450 μg of sCA, and ~2.5 μg of ^{111}In-DOTA-biotin. Blood samples were obtained for kinetic studies. At 2, 19, 52, 104, and 144 h, groups of mice (n = 5) were killed and their organ radioactivity was measured. %ID/g for blood and various organs was calculated and T/NT ratio from 2 to 144 h after ^{111}In-DOTA-biotin injection was presented for each organ as arithmetic mean ± SEM.

(SKNLP, SKNJD, LAN-1) as well as C57Bl/6 mice autografted with GD2-negative melanoma (B16), and GD2-positive melanomas (B16D14, B16D14Kb, B16D14KbKd) were studied using 900 μg of 5F11-scFv-SA, 20–28 h after injection of ^{111}In-DOTA-biotin (Table 6). As expected, GD2-negative tumors had generally low T/NT ratios. However, for the blood compartment or organs with a substantial blood component (e.g., spine and femur), high tumor-to-

TABLE 5
Absorbed Radiation Dose (cGy/MBq) Assuming Complete Local β-Ray Absorption or Using Equal Spheric Organ Mass Assumption

Tissue	Model 1: assuming complete local β-ray absorption			Model 2: using equal spheric organ mass assumption	
	^{90}Y-DOTA-biotin 5F11-scFv-SA (μg)			^{90}Y-DOTA-biotin 5F11-scFv-SA (μg)	
	300	900	^{131}I-3F8	300	900
Bladder	1.9 ± 0.3	4.1 ± 0.6	8.5 ± 1.8	0.4 ± 0.1	0.8 ± 0.1
Blood	1.3 ± 0.6	0.9 ± 0.6	89.2 ± 37.2	NA	NA
Bone	0.9 ± 0.0	1.1 ± 0.2	8.7 ± 1.4	NA	NA
Brain	0.8 ± 0.2	0.9 ± 0.1	3.1 ± 1.3	0.5 ± 0.1	0.5 ± 0.0
Heart	1.2 ± 0.2	1.4 ± 0.2	23.6 ± 2.1	0.6 ± 0.1	0.8 ± 0.1
Kidney	30.6 ± 4.8	50.4 ± 6.7	18.0 ± 3.1	16.1 ± 2.5	26.5 ± 3.5
Large intestine	4.5 ± 0.5	14.6 ± 2.2	7.1 ± 1.1	3.4 ± 0.3	10.8 ± 1.6
Liver	5.1 ± 0.7	7.2 ± 0.2	12.4 ± 2.4	3.9 ± 0.5	5.6 ± 0.2
Lung	3.2 ± 1.4	5.2 ± 1.0	28.6 ± 3.4	1.6 ± 0.7	2.7 ± 0.5
Small intestine	1.1 ± 0.3	1.8 ± 0.6	10.7 ± 0.2	0.9 ± 0.2	1.4 ± 0.5
Spleen	2.1 ± 0.2	2.3 ± 0.2	17.9 ± 1.3	1.1 ± 0.1	1.2 ± 0.1
Stomach	1.5 ± 0.3	1.4 ± 0.2	10.2 ± 6.0	0.8 ± 0.1	0.7 ± 0.1
Tumor	77.0 ± 11.2	153.1 ± 8.3	237.4 ± 40.4	64.5 ± 9.4	128.1 ± 7.0

NA = organ masses were not available for these calculations.
Absorbed radiation dose was calculated and is presented as mean ± SD. Model 1 assumes complete local β-ray absorption: Bladder absorbed dose was calculated without using dynamic bladder model. For walled organs (bladder, large intestine, small intestine, stomach), absorbed dose was calculated based on cpm of organs containing their respective contents. Model 2 uses spheric organ mass assumption: For ^{131}I, there was nearly complete local absorption of β-radiation and correction was not necessary.

TABLE 6
Relationship of T/NT Ratio and Tumors with Different GD2 Expression

	GD2-negative cell line					GD2-positive murine cell line					GD2-positive human cell line			
	H	H	H	M		H	M	M	M		H	H	H	
Tissue	Colo205	Daudi	HTB82	B16	Mean ± SEM*	MOLT-4	B16D14	B16D14Kb	B16D14KbKd	Mean ± SEM*	SK-N-LP	SK-N-JD	LAN-1	Mean ± SEM*
Adrenal	7	1	5	4	4.1 ± 1.4	3	24	11	28	16.4 ± 5.8	245	91	74	136.7 ± 54.5
Bladder	10	1	3	2	4.1 ± 2.0	3	10	2	22	9.2 ± 4.5	162	85	97	114.4 ± 24.0
Blood	6	11	72	28	29.2 ± 14.9	30	169	33	190	105.4 ± 43.1	667	701	442	603.6 ± 81.3
Brain	59	37	43	64	50.7 ± 6.4	66	294	100	427	222.0 ± 85.0	541	1,919	929	1,129.9 ± 410.4
Femur	9	4	18	7	9.6 ± 3.0	7	38	14	52	27.9 ± 10.6	342	741	221	434.9 ± 157.1
Heart	7	2	8	6	5.6 ± 1.4	8	23	8	30	17.5 ± 5.7	231	244	190	221.6 ± 16.2
Kidney	0	0	0	0	0.2 ± 0.1	0	1	0	1	0.5 ± 0.2	5	6	5	5.2 ± 0.3
Large intestine	0	1	1	0	0.9 ± 0.3	0	2	0	2	1.3 ± 0.6	15	12	31	19.4 ± 6.1
Liver	1	0	1	1	1.2 ± 0.3	2	7	3	6	4.3 ± 1.3	59	37	37	44.4 ± 7.5
Lung	2	1	1	1	1.3 ± 0.4	1	3	2	6	3.2 ± 1.1	29	73	41	48 ± 13.3
Muscle	12	6	16	14	11.8 ± 2.3	8	40	16	80	35.9 ± 16.2	451	425	225	366.9 ± 71.5
Skin	1	1	4	2	2.0 ± 0.8	1	7	3	21	8.2 ± 4.7	32	72	73	59.1 ± 13.5
Small intestine	4	3	7	5	4.8 ± 0.9	2	16	2	45	16.2 ± 10.3	174	243	197	204.6 ± 20.1
Spine	10	4	19	9	10.5 ± 3.1	10	36	15	45	26.6 ± 8.4	330	376	131	279.3 ± 75.2
Spleen	3	1	3	2	2.2 ± 0.4	3	10	4	15	8.1 ± 2.9	174	120	71	122 ± 29.7
Stomach	3	3	21	3	7.7 ± 4.4	7	20	5	42	18.6 ± 8.5	109	197	784	363.4 ± 211.6
GD2 (%LAN-1)†	2	4	3	4	3.3 ± 0.5	17	22	32	12	20.8 ± 4.3	289	77	100	155.4 ± 67.2

*Mean ± SEM = arithmetic mean ± SEM across cell lines in each tumor group.

†GD2 (% LAN-1) = relative mean fluorescence, indirect fluorescent staining with anti-GD2 antibody 3F8. It is calculated as mean fluorescence channel of cell line divided by mean fluorescence channel of NB cell line LAN-1.

H = human, M = murine.

Mice (n = 4 or 5 per group) xenografted with GD2-negative human lymphoma (Daudi), leukemia (MOLT-4), colon carcinoma (Colo205), rhabdomyosarcoma (HTB82), and GD2-positive NB (SK-N-LP, SK-N-JD, LAN-1) as well as C57Bl/6 mice autografted with GD2-negative melanoma (B16), and GD2-positive melanomas (B16D14, B16D14Kb, B16D14KbKd) were studied using 900 μg of 5F11-scFv-SA, 450 μg of sCA, and ~2.5 μg of ^{111}In-DOTA-biotin. At 20–28 h, mice were killed and their organ radioactivity was measured. %ID/g for blood and various organs was calculated and T/NT ratio was presented for each organ.

tissue ratios were most likely a result of active removal by the sCA. The tumor-to-brain ratio was a consequence of the blood–brain barrier, not specific targeting. In general, the average T/NT ratio correlated with the level of positivity (mean fluorescence) of the tumors when assayed by flow cytometry.

5F11-scFv-SA MST for Targeting Small Peptides and Proteins

MST was performed in LAN-1 xenografted athymic nude mice. Instead of ^{111}In-DOTA-biotin, ^{125}I-labeled biotinylated peptides (VIP and PHI, Fig. 4) as well as ^{125}I-labeled biotinylated BSA were administered. VIP is a 28-amino-acid human neuropeptide with immunoregulatory functions (*28*), whereas PHI is a 27-amino-acid porcine intestinal peptide with biologic activities similar to those of VIP. Mice were then imaged at 24, 48, and 120 h after injection. Biodistribution was performed at 48 h (Table 7). VIP, PHI, and BSA showed no selective tumor uptake without MST. In contrast, biotinylated VIP, PHI, and BSA showed selective tumor uptake after pretargeting with 5F11-scFv-SA.

DISCUSSION

Using anti-GD2 scFv-SA in MST to tumor xenografts and autografts, we achieved a tumor-to-blood or T/NT ratio superior to single-step IgG targeting. This favorable ratio was evident at all time points after radioligand injection and translated into a tumor exposure (area under the curve for tumor [AUC_{tumor}]) versus blood exposure (AUC_{blood}) of >150, representing a >50-fold improvement over whole IgG targeting. Tumor uptake at 2 h was 7 %ID/g, and decayed with a $t_{1/2}$ of 72 h, whereas blood %ID/g rapidly decreased to <1/500 of the tumor %ID/g after the first 24 h. Despite the large improvement in the tumor-to-blood or T/NT ratio, nonspecific renal uptake was observed when small ligands were used. The early uptake in the intestines was attributed to the special chow the mice ate, which contained substantial amounts of avidin to prevent biotin from being absorbed. We have shown that the MST strategy was efficient in delivering biotinylated peptides and BSA in a highly tumor-selective fashion, providing the proof of principle that this MST strategy may be applicable to other

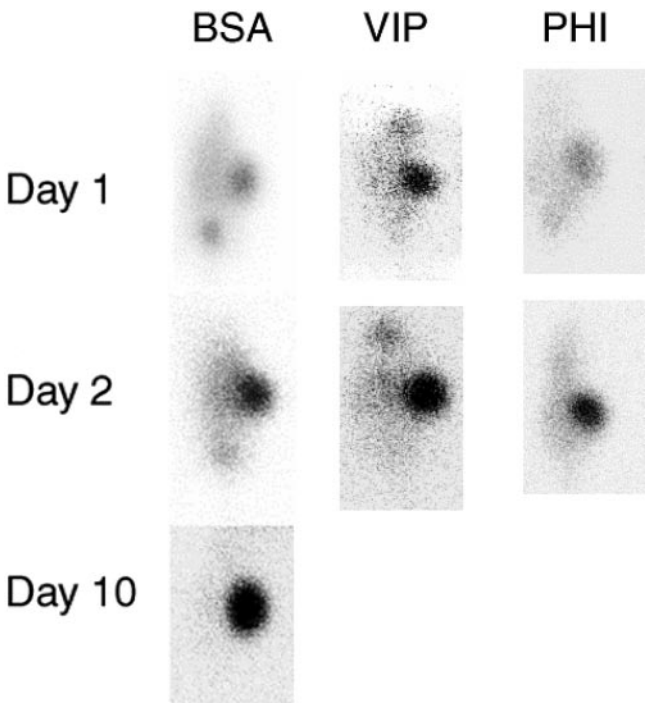

FIGURE 4. 5F11-scFv-SA MST to target peptides and proteins. MST was performed in LAN-1 xenografted athymic nude mice. Instead of ^{111}In-DOTA-biotin, ^{125}I-labeled biotinylated BSA or ^{125}I-labeled biotinylated peptides (VIP and PHI) were administered. Mice were then imaged at 24 and 48 h after injection. Only for the BSA group was there enough retention of radioactivity in tumor at 120 h to allow scintigraphy. No selective tumor uptake was found in biodistribution when radiolabeled BSA, VIP, and PHI were administered alone without MST.

biotinylated ligands. Both AUC improvement and broad ligand applicability represent possibilities of MST not previously explored. Given the relative robustness of targeting at various doses of the components of MST, manipulating the ligand dose to increase tumor uptake of DOTA-biotin is worthy of further investigation.

Using a chemical conjugate of mAb NR-LU-10 and streptavidin followed by galactosyl-HSA as the sCA, ^{90}Y was delivered by DOTA-biotin to effect cures in established xenografts (human small cell lung cancer, colon, and breast cancer models) (*20*) with minimal toxicities. In phase I and II studies in patients with adenocarcinomas, MST using this antibody achieved a favorable tumor-to-marrow absorbed-dose ratio, with some toxicities reported primarily on marrow, gastrointestinal tract, and kidneys, plus an encouraging tumor response (*29*,*30*). Similar successes were reported for MST in other preclinical models (*17*,*31*,*32*) and patient studies (*33*,*34*). A transient antistreptavidin immune response was seen in the majority of patients (*29*,*33*), although it was generally delayed (up to 8 wk). Other strategies using bispecific antibodies that recognize tumor and chelating agents (1,4,8,11-tetraazacyclotetradecane-1,4,8,11-tetraacetic acid [TETA], DOTA, diethylenetriaminepentaacetic acid) have also been explored with promising results (*14*,*35*,*36*).

Despite the high density of the GD2 antigen on tumor targets and the molecular size of the 5F11-scFv-SA being 172 kDa, the %ID/g observed in our studies was suboptimal. A likely explanation was the faster clearance of 5F11-scFv-SA in our tumor model compared with B9E9-SA and

TABLE 7
MST of VIP, PHI, and BSA: T/NT Ratio at 48 Hours

Tissue	VIP		PHI		BSA	
	MST	None	MST	None	MST	None
Adrenal	24.5 ± 8.2	4 ± 0.8	87.5 ± 11.6	3.8 ± 1.7	26.8 ± 7.8	1.3 ± 0.2
Bladder	31.5 ± 6.6	2.4 ± 0.9	53.9 ± 20	2.4 ± 0.9	36.5 ± 5.2	2.1 ± 0.8
Blood	26.6 ± 3.3	1.7 ± 0.2	32 ± 4.9	2.1 ± 0.9	10.8 ± 0.9	0.7 ± 0.1
Brain	209 ± 42.8	13.4 ± 4.6	251 ± 26.6	14.5 ± 6.9	101 ± 7.9	13.4 ± 2.2
Femur	39.9 ± 6.1	3.4 ± 0.3	71.5 ± 6.7	5.1 ± 2.7	59.4 ± 23.2	4.9 ± 2.4
Heart	36.5 ± 4.7	2.5 ± 0.2	58.4 ± 3.5	3.6 ± 1.5	16.7 ± 1.5	1.6 ± 0.3
Kidney	1.1 ± 0.2	0.1 ± 0	3.6 ± 1.1	0.1 ± 0	11.8 ± 0.9	1.2 ± 0.2
Large intestine	6.5 ± 0.5	0.6 ± 0.2	5 ± 0.9	0.7 ± 0.6	9.3 ± 1.8	0.7 ± 0.2
Liver	6.9 ± 1.1	0.5 ± 0.1	13.8 ± 2.5	0.6 ± 0.2	5.7 ± 0.7	0.8 ± 0.2
Lung	9.1 ± 1.4	0.7 ± 0.3	17.9 ± 4.4	0.8 ± 0.3	9.6 ± 0.7	0.6 ± 0.1
Muscle	83.3 ± 10.3	6.1 ± 1.2	96.1 ± 13	6.1 ± 2.5	75.6 ± 11.4	5 ± 1.1
Skin	9.8 ± 1	1.3 ± 0.7	14.8 ± 2	1.4 ± 0.7	20.8 ± 4.1	1.7 ± 0.4
Small intestine	33.4 ± 4.6	2.7 ± 0.2	47 ± 7.6	2.8 ± 1.1	25.7 ± 6.4	1.8 ± 0.4
Spine	56 ± 9.2	2.9 ± 0.2	79.5 ± 7	6.3 ± 3.2	30.5 ± 1.9	2.3 ± 0.3
Spleen	9.8 ± 1.9	1.2 ± 0.2	37.4 ± 8.3	2.6 ± 1.3	5 ± 0.7	2.1 ± 0.5
Stomach	4.7 ± 1	0.4 ± 0.2	5.3 ± 1.4	0.8 ± 0.4	8.8 ± 3	0.5 ± 0.2

T/NT ratio was calculated as follows: (%ID/g in tumor)/(%ID/g in tissue). Athymic mice (n = 5–10 per group) with xenografted NB LAN-1 were injected with standard dose of 900 μg of 5F11-scFv-SA, 450 μg of sCA, and ^{125}I-labeled VIP, PHI, or BSA. Blood samples were obtained for kinetic studies. At 48 h, mice were killed and their organ radioactivity was measured. %ID/g for blood and various organs was calculated and T/NT ratio was expressed as mean ± SEM.

CC49-scFv-SA. Shedding of GD2 from rapidly growing NB has been reported in patients with advanced disease and is one potential explanation for our observation in mice studies. Alternatively, 5F11-scFv-SA may dissociate in plasma-forming dimers or monomers of smaller molecular size. Although molecular sizing studies did not show dissociation of 5F11-scFv-SA in plasma (data not shown), we could not entirely rule out this possibility unless the tetrameric form was chemically stabilized. Another possibility could relate to the inherent amino acid sequence of the particular scFv-fusion protein, which can affect its in vivo biodistribution properties (*37*).

For most genetic fusion proteins, immunogenicity can pose a significant obstacle to retreatment. Streptavidin is a bacterial protein without a mammalian analog and thus cannot be humanized. Previous attempts to decrease its immunogenicity has largely failed, including PEGylation, which unfortunately decreased its affinity for biotin (*38*). Most patients with NB do not develop human antimouse antibody response despite repeated challenges, often for as long as 6–12 mo after completion of induction chemotherapy with or without myeloablative therapy. This window of slow immune recovery is also the risk period for NB recurrence, when targeted therapy can most likely be optimally applied. However, given the immunogenicity of streptavidin, it is not surprising that a substantial percentage of patients with non-Hodgkin's lymphoma treated with anti-CD20-streptavidin developed an immune response to the fusion protein. Whether patients with NB will develop similar immune response early after streptavidin injection may have to await the results of the clinical trial.

CONCLUSION

The T/NT uptake ratio can be greatly improved using pretargeting strategy directed at ganglioside GD2, thereby increasing the efficacy and safety of scFv-based cancer radioimmunoscintigraphy and radioimmunotherapy. In addition, since biotinylated polypeptides can be rendered tumor selective, a large repertoire of agents besides radiolabeled ligands can potentially be explored. Although tumor-to-blood targeting ratio was favorable, the renal trapping of scFv fusion proteins or biotinylated ligands would require future optimization.

ACKNOWLEDGMENT

This study was supported in part by grants from the Department of Energy (ER61658 and ER 86039), the Robert Steel Foundation, and the National Institutes of Health (CA61017 and Small Animal Imaging Resource Program R24 CA83084).

REFERENCES

1. Rodden FA, Wiegandt H, Bauer BL. Gangliosides: the relevance of current research to neurosurgery. *J Neurosurg.* 1991;74:606–619.
2. Larson SM, Divgi C, Sgouros G, Cheung NKC, Scheinberg DA. Monoclonal antibodies: basic principles—adioisotope conjugates. In: DeVita VT, Hellman S, Rosenberg SA, eds. *Biologic Therapy of Cancer: Principles and Practice.* Philadelphia, PA: JB Lippincott; 2000:396–412.
3. Cheung NK, Saarinen U, Neely J, Landmeier B, Donovan D, Coccia P. Monoclonal antibodies to a glycolipid antigen on human neuroblastoma cells. *Cancer Res.* 1985;45:2642–2649.
4. Honsik CJ, Jung G, Reisfeld RA. Lymphokine-activated killer cells targeted by monoclonal antibodies to the disialogangliosides GD2 and GD3 specifically lyse human tumor cells of neuroectodermal origin. *Proc Natl Acad Sci USA.* 1986; 83:7893–7897.
5. Cheung NK, Kushner BH, Kramer K. Monoclonal antibody-based therapy of neuroblastoma. *Hematol Oncol Clin North Am.* 2001;15:853–866.
6. Huston JS, Levinson D, Mudgett-Hunter M, et al. Protein engineering of antibody binding sites: recovery of specific activity in an anti-digoxin single-chain Fv analogue produced in Escherichia coli. *Proc Natl Acad Sci USA.* 1988;85:5879–5883.
7. Bird RE, Hardman KD, Jacobson JW, et al. Single-chain antigen-binding proteins. *Science.* 1988;242:423–426.
8. Kipriyanov SM, Bretling F, Little M, Dubel S. Single-chain antibody streptavidin fusions: tetrameric bifunctional scFv-complexes with biotin binding activity and enhanced affinity to antigen. *Hum Antibodies Hybridomas.* 1995;6:93–101.
9. Zhang M, Zhang Z, Garmestani K, et al. Pretarget radiotherapy with an anti-CD25 antibody-streptavidin fusion protein was effective in therapy of leukemia/lymphoma xenografts. *Proc Natl Acad Sci USA.* 2003;100:1891–1895.
10. Hnatowich DJ, Virzi F, Rusckowski M. Investigations of avidin and biotin for imaging applications. *J Nucl Med.* 1987;28:1294–1302.
11. Paganelli G, Malcovati M, Fazio F. Monoclonal antibody pretargetting techniques for tumour localization: the avidin-biotin system: International Workshop on Techniques for Amplification of Tumour Targetting. *Nucl Med Commun.* 1991;12:211–234.
12. Goodwin DA, Meares CF. Pretargeting: general principles—October 10–12, 1996. *Cancer.* 1997;80(12 suppl):2675–2680.
13. Theodore LJ, Fritzberg AR, Schultz JE, Axworthy DB. Evolution of a pretarget radioimmunotherapeutic regimen. In: Abrams PG, Fritzberg AR, eds. *Radioimmunotherapy of Cancer.* New York, NY: Marcel Dekker; 2000:195–221.
14. Goldenberg DM. Advancing role of radiolabeled antibodies in the therapy of cancer. *Cancer Immunol Immunother.* 2003;52:281–296.
15. Cheung NK, Guo HF, Modak S, Cheung IY. Anti-idiotypic antibody facilitates scFv chimeric immune receptor gene transduction and clonal expansion of human lymphocytes for tumor therapy. *Hybrid Hybridomics.* 2003;22:209–218.
16. Guo HF, Rivlin K, Dubel S, Cheung NKV. Recombinant anti-ganglioside GD2 scFv-streptavidin fusion protein for tumor pretargeting [abstract]. *Proc Am Assoc Cancer Res.* 1996;37:469.
17. Schultz J, Lin Y, Sanderson J, et al. A tetravalent single-chain antibody-streptavidin fusion protein for pretargeted lymphoma therapy. *Cancer Res.* 2000;60: 6663–6669.
18. Cheung NK, Guo HF, Modak S, Cheung IY. Anti-idiotypic antibody as the surrogate antigen for cloning scFv and its fusion proteins. *Hybrid Hybridomics.* 2002;21:433–443.
19. Theodore L, Axworthy D, inventors; NeoRx Corporation, assignee. Cluster clearing agents. US patent 6 172 045. January 9, 2001.
20. Axworthy DB, Reno JM, Hylarides MD, et al. Cure of human carcinoma xenografts by a single dose of pretargeted yttrium-90 with negligible toxicity. *Proc Natl Acad Sci USA.* 2000;97:1802–1807.
21. Cheung NK, Landmeier B, Neely J, et al. Complete tumor ablation with iodine 131-radiolabeled disialoganglioside GD2-specific monoclonal antibody against human neuroblastoma xenografted in nude mice. *J Natl Cancer Inst.* 1986;77: 739–745.
22. Boston RC, Weiss M, Shahn E. Conversational SAAM: an interactive program for kinetic analysis of biological systems. *Comput Programs Biomed.* 1981;13: 1111–1119.
23. Zanzonico P, Poston JW. Computational methods in internal radiation dosimetry. In: Zaidi H, Sgouros G, eds. *Monte Carlo Calculations in Nuclear Medicine: Therapeutic Applications.* Bristol, U.K.: IOP Publishing Ltd.; 2002:84–108.
24. Stabin MG, Konijnenberg MW. Re-evaluation of absorbed fractions for photons and electrons in spheres of various sizes. *J Nucl Med.* 2000;41:149–160.
25. Kolbert KS, Watson T, Matei C, Xu S, Koutcher JA, Sgouros G. Murine S factors for liver, spleen, and kidney. *J Nucl Med.* 2003;44:784–791.
26. Cheung NK, Neely JE, Landmeier B, Nelson D, Miraldi F. Targeting of ganglioside GD2 monoclonal antibody to neuroblastoma. *J Nucl Med.* 1987;28:1577–1583.
27. Ugur O, Kostakoglu L, Hui ET, et al. Comparison of the targeting characteristics of various radioimmunoconjugates for radioimmunotherapy of neuroblastoma:

dosimetry calculations incorporating cross-organ beta doses. *Nucl Med Biol.* 1996;23:1–8.
28. Ganea D, Delgado M. Vasoactive intestinal peptide (VIP) and pituitary adenylate cyclase-activating polypeptide (PACAP) as modulators of both innate and adaptive immunity. *Crit Rev Oral Biol Med.* 2002;13:229–237.
29. Breitz HB, Weiden PL, Beaumier PL, et al. Clinical optimization of pretargeted radioimmunotherapy with antibody-streptavidin conjugate and ^{90}Y-DOTA-biotin. *J Nucl Med.* 2000;41:131–140.
30. Knox SJ, Goris ML, Tempero M, et al. Phase II trial of yttrium-90-DOTA-biotin pretargeted by NR-LU-10 antibody/streptavidin in patients with metastatic colon cancer. *Clin Cancer Res.* 2000;6:406–414.
31. Press OW, Corcoran M, Subbiah K, et al. A comparative evaluation of conventional and pretargeted radioimmunotherapy of CD20-expressing lymphoma xenografts. *Blood.* 2001;98:2535–2543.
32. Zhang M, Yao Z, Garmestani K, et al. Pretargeting radioimmunotherapy of a murine model of adult T-cell leukemia with the alpha-emitting radionuclide, bismuth 213. *Blood.* 2002;100:208–216.
33. Weiden PL, Breitz HB, Press O, et al. Pretargeted radioimmunotherapy (PRIT) for treatment of non-Hodgkin's lymphoma (NHL): initial phase I/II study results. *Cancer Biother Radiopharm.* 2000;15:15–29.
34. Paganelli G, Bartolomei M, Ferrari M, et al. Pre-targeted locoregional radioimmunotherapy with ^{90}Y-biotin in glioma patients: phase I study and preliminary therapeutic results. *Cancer Biother Radiopharm.* 2001;16:227–235.
35. DeNardo SJ, DeNardo GL, DeNardo DG, et al. Antibody phage libraries for the next generation of tumor targeting radioimmunotherapeutics. *Clin Cancer Res.* 1999;5(10 suppl):3213s–3218s.
36. Boerman OC, Kranenborg MH, Oosterwijk E, et al. Pretargeting of renal cell carcinoma: improved tumor targeting with a bivalent chelate. *Cancer Res.* 1999; 59:4400–4405.
37. Onda M, Nagata S, Tsutsumi Y, et al. Lowering the isoelectric point of the Fv portion of recombinant immunotoxins leads to decreased nonspecific animal toxicity without affecting antitumor activity. *Cancer Res.* 2001;61:5070–5077.
38. Chinol M, Casalini P, Maggiolo M, et al. Biochemical modifications of avidin improve pharmacokinetics and biodistribution, and reduce immunogenicity. *Br J Cancer.* 1998;78:189–197.

JNM The Journal of NUCLEAR MEDICINE

Single-Chain Fv-Streptavidin Substantially Improved Therapeutic Index in Multistep Targeting Directed at Disialoganglioside GD2

Nai-Kong V. Cheung, Shakeel Modak, Yukang Lin, Hongfen Guo, Pat Zanzonico, John Chung, Yuting Zuo, James Sanderson, Sibylle Wilbert, Louis J. Theodore, Donald B. Axworthy and Steven M. Larson

J Nucl Med. 2004;45:867-877.

The Journal of Nuclear Medicine is published monthly.
SNMMI | Society of Nuclear Medicine and Molecular Imaging
1850 Samuel Morse Drive, Reston, VA 20190.
(Print ISSN: 0161-5505, Online ISSN: 2159-662X)

SNMMI SOCIETY OF NUCLEAR MEDICINE AND MOLECULAR IMAGING